Title:

Cannabinoid signalling inhibits sarcoplasmic Ca^{2+} release and regulates excitation-contraction coupling in mammalian skeletal muscle

Running title:

CB1 receptors and SR calcium release

Authors:

Tamás Oláh[a], Dóra Bodnár[a], Adrienn Tóth[a], János Vincze[a], János Fodor[a], Barbara Reischl[b], Adrienn Kovács[a], Olga Ruzsnavszky[a], Beatrix Dienes[a], Péter Szentesi[a], Oliver Friedrich[b], László Csernoch[a,1]

Affiliations:

[a] Department of Physiology, Faculty of Medicine, University of Debrecen, 4032, Debrecen, Hungary

[b] Institute of Medical Biotechnology, Friedrich-Alexander-University Erlangen-Nürnberg, 91052, Erlangen, Germany

[1] **Corresponding author:**

Dr. László Csernoch

Department of Physiology, Faculty of Medicine, University of Debrecen

Hungary, H-4032, Debrecen, Egyetem tér 1.

E-mail: csl@edu.unideb.hu

Fax: +36-52-255-116

KEY POINTS SUMMARY

- Marijuana was found to cause muscle weakness, but the exact regulatory role of its receptors – CB1 cannabinoid receptors (CB1R) – in excitation-contraction coupling (ECC) of mammalian skeletal muscle is yet unknown.
- We found that CB1R activation or its knockout did not affect muscle force directly, while its activation decreased the Ca^{2+}-sensitivity of the contractile apparatus and made the muscle fibres more prone to fatigue.
- We demonstrate that neither in myotubes nor in adult muscle fibres are CB1Rs connected to the IP_3 pathway.
- On the other hand, CB1Rs constitutively inhibit sarcoplasmic Ca^{2+} release and sarcoplasmic reticulum Ca^{2+} ATPase during ECC in a $G_{i/o}$ protein mediated way in adult skeletal muscle fibres, but not in myotubes.
- These results help us understand the physiological effects and pathological consequences of CB1R activation in skeletal muscle and can be useful for the development of new cannabinoid drugs.

ABSTRACT

Marijuana was found to cause muscle weakness, but it is unknown whether it affects the muscles directly, or modulates only the motor control of the central nervous system. Although the presence of CB1 cannabinoid receptors (CB1R) – responsible for the psychoactive effects of the drug in the brain – have recently been shown in skeletal muscle, it is unclear how CB1R-mediated signalling affects the contraction and Ca^{2+} homeostasis of mammalian skeletal muscle. Here we demonstrate that *in vitro* CB1R activation increased muscle fatigability, decreased the Ca^{2+}-sensitivity of the contractile apparatus, but did not alter the amplitude of single twitch contractions. In myotubes, CB1R agonists neither evoked or influenced IP_3-mediated Ca^{2+} transients, nor altered excitation-contraction coupling. In contrast, in isolated muscle fibres of wild type mice, although CB1R agonists did not evoke IP_3-mediated Ca^{2+} transients too, they significantly reduced the amplitude of the depolarization-evoked transients in a pertussis-toxin sensitive way, indicating a $G_{i/o}$ protein dependent mechanism. Concurrently, on skeletal muscle fibres isolated from CB1R-knockout animals,

depolarization-evoked Ca^{2+} transients, Ca^{2+} release flux via ryanodine receptors (RyRs), and total amount of released Ca^{2+} was significantly greater than those from wild type mice. Our results show that CB1R-mediated signalling exerts both a constitutive and an agonist-mediated inhibition on the Ca^{2+} transients via RyR, regulates the activity of the sarcoplasmic reticulum Ca^{2+} ATPase, and enhances muscle fatigability, which might decrease exercise performance, play a role in myopathies, and should, therefore, be considered during the development of new cannabinoid drugs.

KEYWORDS:
CB1 cannabinoid receptor, skeletal muscle, calcium transient, contraction, KO mouse

ABBREVIATIONS. 4-CMC, 4-chloro-m-cresol; $[Ca^{2+}]_i$, intracellular calcium concentration; $[Ca^{2+}]_T$, total amount of calcium released; ACEA, arachidonyl-2'-chloroethylamide; AEA, anandamide (N-arachidonoyl ethanolamine); CaV, voltage-gated Ca^{2+} channel; CB1R, cannabinoid receptor type 1; CB2R, cannabinoid receptor type 2; DHPR, dihydropyridine receptor; ECC, excitation-contraction coupling; EDL, *extensor digitorum longus*; FDB, *flexor digitorum brevis*; FKBP12, FK-506 binding protein; IP_3, inositol 1,4,5-trisphosphate; KO: CB1R-knockout; PKA, protein kinase A; PLB, phospholamban; PKI, PKI 14-22 amide, myristoylated; PTX, pertussis toxin; PV_{max}, maximal transport rate of the Ca^{2+} pump; RyR, ryanodine receptor; SERCA, sarco/endoplasmic reticulum Ca^{2+} ATPase; SLN, sarcolipin; SOCE, store-operated Ca^{2+} entry; Sol, soleus; SR, sarcoplasmic reticulum; STIM1, stromal interaction molecule type 1; WIN, WIN55,212-2 (*R*)-(+)-[2,3-Dihydro-5-methyl-3-(4-morpholinylmethyl)pyrrolo[1,2,3-*de*]-1,4-benzoxazin-6-yl]-1-naphthalenylmethanone mesylate; WT, wild type

1. INTRODUCTION

The receptors of the psychoactive compound of marijuana can also be activated by endogenous ligands (e.g. anandamide (Devane et al. 1992) and 2-arachidonoyl glycerol). These ligands are produced, detected and degraded by the endocannabinoid system (Pertwee et al. 2010). The main cannabinoid receptor – CB1 receptor (CB1R) – is present both in neural and peripheral tissues (Pertwee et al. 2010; Maccarrone et al. 2015), and can connect to different G proteins ($G_{i/o}$, G_q, and G_s), depending on the cell type (Lauckner et al. 2005; Turu and Hunyady 2010). This ubiquity and versatility enables a wide variety of regulatory functions, e.g. motor coordination, memory, appetite, pain modulation, neuroprotection, cognitive functions, affective states, and maintenance of energy homeostasis (Fišar et al. 2014). Inhibition of the endocannabinoid system by neutral CB1R antagonists in the peripheral organs is among the most promising ways to treat obesity, while the activation of CB1Rs (by e.g. medical marijuana) in the nervous system can be used to treat nausea, vomiting, anorexia, weight loss, muscle spasms, and pain (Pacher and Kunos 2013; Borgelt et al. 2013). Thus, in the organs responsible for these effects, the role of CB1Rs is extensively studied. However, there are organs in which the physiological role of the cannabinoid system is much less understood.

The skeletal muscle system comprises 30-40% of the body mass in humans. It is responsible for all the voluntary movements, and it is also a key player in glucose metabolism (Sinacore and Gulve 1993) and thermoregulation (Rowland et al. 2015) of the body. The expression of CB1 and CB2 cannabinoid receptors and the enzymes responsible for the synthesis (N-acyl phosphatidylethanolamine-selective phospholipase D, diacylglycerol lipase α and β) and degradation (fatty acid amide hydrolase, monoacylglycerol lipase) of the endocannabinoid compounds has recently been demonstrated in mammalian skeletal muscle (Cavuoto et al. 2007; Crespillo et al. 2011; Hutchins-Wiese et al. 2012). By now, the role of cannabinoid signalling in glucose uptake and energy balance of the muscle has been well described: inhibition of CB1R decreases insulin resistance (Taube et al. 2009), augments glucose uptake (Lindborg et al. 2010) and decreases body weight (Crespillo et al. 2011) in a protein kinase A (PKA)

dependent way by stimulating the expression and activity of phosphatidylinositol-3-kinase (Esposito et al. 2008) and extracellular signal-regulated kinase 1/2 (Lipina et al. 2010). In myogenesis, the role of CB1R activation was also shown: it decreases myoblast differentiation via inhibition of Kv7.4 channels (Iannotti et al. 2014).

However, surprisingly, in the regulation of the main and most obvious function of skeletal muscle – contraction – the exact role of the cannabinoid system still awaits clarification. Cannabinoids were found to affect muscle activity, but it was not investigated whether they acted on the muscles directly, or affected them indirectly, solely by modulating their nervous control. In these studies, smoking marijuana caused muscle weakness (Lorente Fernandez et al. 2014) and muscle fatigue (Renaud and Cormier 1986) in human patients, and activation of CB1Rs decreased, while their inhibition increased the locomotor activity of treated mice (Zimmer et al. 1999). To our knowledge, there is only one study where it was unequivocally shown that the tested cannabinoids acted directly on the muscles, but this study was performed on frog muscles, and its transferability to human physiology is limited. There, CB1R agonists attenuated the caffeine-induced force transients (Huerta et al. 2009). Thus, there is a need for related results on clinically more relevant mammalian experimental models. Moreover, if cannabinoids directly altered contractile force or fatigue of mammalian muscles, this would point to a yet uninvestigated adverse effect or even a new target for cannabinoid drug development. Furthermore, since there is an unexpectedly high rate (>25%) of marijuana use among student athletes (Buckman et al., 2011), knowing how marijuana smoking affects exercise performance could be a strong argument for the future success of drug prevention.

If the above mentioned fatigue and weakness originated directly in the muscle, one might hypothesize that CB1R activation regulates excitation-contraction coupling (ECC) by a yet unknown mechanism. ECC is a process during which the depolarization of the plasma membrane activates dihydropyridine receptors (DHPR) that mechanically couple to ryanodine receptors (RyR) to release Ca^{2+} from the sarcoplasmic reticulum (SR) required for muscle contraction (Franzini-Armstrong and Protasi 1997). To enable muscle relaxation, Ca^{2+} is subsequently re-uptaken by the sarco/endoplasmic reticulum Ca^{2+} ATPase (SERCA) (Stammers et al. 2015). However, it is unclear yet, which step of ECC is affected by the CB1R mediated signalling. In skeletal muscle, even the

immediate downstream signalling partners of CB1Rs are highly debated. In some cell types, CB1R is connected to G_q proteins and the inositol 1,4,5-trisphosphate (IP_3) pathway, causing an elevation of intracellular calcium concentration ($[Ca^{2+}]_i$) (Navarrete and Araque 2008; Lauckner et al. 2005), and the same was proposed for skeletal myoblast cell cultures in a recent study (Iannotti et al. 2014). In contrast, in another study, the effects of CB1R activation in frog skeletal muscle were assumed to be mediated by a $G_{i/o}$ protein dependent way (Huerta et al. 2009), similar to the majority of other studies performed on various non-muscle cell types (Turu and Hunyady 2010). The exact steps of the signalling cascade by which CB1Rs affect muscle force and Ca^{2+} homeostasis in adult mammalian skeletal muscle fibres, are also yet to be discovered.

In this study, we aimed to decipher the signalling pathways and to understand the role played by CB1Rs in muscle performance, contractions and Ca^{2+} homeostasis using a CB1R-knockout animal model, applying *in vivo* muscle performance tests, *in vitro* force measurements, single-cell Ca^{2+} imaging, confocal microscopy, and biochemical techniques. Our results indicate that CB1Rs localize around the Z-lines, and constitutively inhibit SR Ca^{2+} release during ECC in a $G_{i/o}$ protein mediated way in adult skeletal muscle fibres, but not in myotubes. Moreover, CB1R activation decreases the Ca^{2+} sensitivity of the contractile proteins and increases muscle fatigue.

2. MATERIALS AND METHODS

2.1. Ethical approval, animal care, CB1R-knockout mice

Animal experiments conformed to the guidelines of the European Community (86/609/EEC) and the institutional Animal Care Committee of University of Debrecen (31/2012/DE MAB). CB1R-knockout (KO) mice were a kind gift from Dr. Andreas Zimmer (Zimmer et al. 1999). 8-10 week-old wild type C57BL/6 (WT) and KO mice were used for the experiments. The mice were housed in plastic cages with mesh covers, and fed with pelleted mouse chow and water *ad libitum*. Room illumination was an automated cycle of 12 h light and 12 h dark, and room temperature was maintained within the range 22–25°C. When necessary, mice were killed by cervical dislocation after anaesthesia with pentobarbital.

2.2 In vivo muscle performance measurements

Voluntary activity wheel measurements, forepaw grip tests and wire hang tests were performed as described previously (Bodnár et al. 2014, Oddoux et al. 2009).

2.3. Measurement of muscle force and fatigability on whole muscles

Muscle contractions of fast *extensor digitorum longus* (EDL) and slow *soleus* (Sol) muscles were measured as described previously (Oddoux et al. 2009). Series of single electric pulses (5 V), 2 s or 4 s apart, were used to elicit single twitches in EDL and Sol muscles, respectively. To elicit a tetanus, single pulses were applied with a frequency of 100 Hz for 200 ms in case of EDL and 50 Hz for 500 ms in case of Sol. Series of tetani were recorded with a frequency of 0.25 trains/s. In a series of stimulation, at least 10 twitches or tetani were measured under these conditions from every muscle; and two consecutive series were compared on each muscle. Between two following series, 5 min of intermittent period was applied for relaxation and recovery of the muscles and for treatment with the CB1R agonist 1 μM WIN55,212-2 (WIN; from Tocris Bioscience, Bristol, UK), both for twitches and tetani.

To test muscle fatigability, 150 tetanic contractions (200 Hz for 200 ms) at a frequency of 0.5 Hz were evoked (Oddoux et al. 2009). The amplitude of each tetanus was normalized to that of the largest in the series (usually the first or the second) and plotted

as a function of the position within the series. In some experiments, WT muscles were pre-treated with 1 μM WIN for 1 hour before and during the measurement.

2.4. Measurement of muscle force in small fibre bundles

Small fibre bundles of five fibres were mechanically isolated from EDL muscles of WT mice. The ends of the bundles were cut which enabled a moderate exchange between the intra- and extracellular solutions. A computer-aided force transducer system based on a KG-7 sensor (MyoTronik, Heidelberg, Germany; similar as in Friedrich et al. 2014) was used to measure isometric contractions of the bundles. Contractions were evoked by dipping the bundles into different solutions using a custom designed, motorized, programmable rack of wells. Experiments were performed at 30 °C. During the measurements, the following solutions were used: high activating solution containing 30 mM caffeine and the maximal physiologically active [Ca^{2+}] for evoking contractures (containing in mM: 30 HEPES, 6.05 $Mg(OH)_2$, 30 EGTA, 29 $CaCO_3$, 8 Na_2ATP, 10 Na_2-creatine phosphate, 1% creatine kinase), high relaxing solution for washout of Ca^{2+} after every Ca^{2+}-containing solutions and to induce relaxation (containing in mM: 30 HEPES, 6.25 $Mg(OH)_2$, 30 EGTA, 8 Na_2ATP, 10 Na_2-creatine phosphate, 1% creatine kinase), and low relaxing solution for washout of high EGTA prior to release, baseline recording, and treatment with 1μM WIN (containing in mM: 30 HEPES, 7.86 $Mg(OH)_2$, 87.7 K-glutamate, 0.4 EGTA, 6.6 HDTA, 8 Na_2ATP, 10 Na_2-creatine phosphate, 1% creatine kinase).

2.5. Ca^{2+} sensitivity of the contractile apparatus

EDL fibre bundles of WT mice were either untreated or treated with 1 μM WIN for 15 min and then chemically skinned with 0.1% saponin for 2 min. Ca^{2+} contractures were evoked by immersing the bundles from a highly-buffered EGTA containing Ca^{2+}-free 'high relaxing solution' to activating solutions (high relaxing solution supplemented with Ca^{2+}) of gradually increasing [Ca^{2+}]. Isometric force values were normalized for the maximal Ca^{2+}-activated active force, and Ca^{2+}–force relationships were plotted to determine the Ca^{2+}-sensitivity of isometric force production. The relationship between force and pCa was fitted with a Hill equation; the Hill coefficient being a measure of the coordinativity and pCa_{50} reflecting the Ca^{2+}-sensitivity.

2.6. Cell cultures

C2C12 cells were cultured using a standard protocol described previously (Oláh et al. 2011). Functional experiments were carried out on 5- to 6-day-old terminally differentiated myotubes.

2.7. Isolation of single skeletal muscle fibres

Experiments were carried out on fibres from the *flexor digitorum brevis* (FDB) muscles of the mice. Single muscle fibres were enzymatically dissociated in calcium free modified Tyrode's solution (in mM: 137 NaCl, 5.4 KCl, 0.5 $MgCl_2$, 11.8 HEPES, pH 7.4; all from Sigma) containing 0.2% Type I collagenase (Sigma) at 37°C for 50-55 minutes (Bodnár et al. 2014), and stored in a refrigerator until further use. To release single fibres, muscles were triturated gently in normal Tyrode's solution (in mM: 137 NaCl, 5.4 KCl, 0.5 $MgCl_2$, 1.8 $CaCl_2$, 11.8 HEPES, 1 g/l glucose, pH 7.4, all from Sigma) containing 1.8 mM $CaCl_2$. The fibres were then mounted on laminin-coated coverslips and used for experiments.

2.8. Immunocytochemistry

FDB fibres were fixed with 2% paraformaldehyde in 50% methanol for 15 min, permeabilized with 0.5% Triton X-100 in PBS for 10 min, and blocked with 0.2% Triton X-100 diluted in Serum-Free Protein Block (Dako, Glostrup, Denmark) for 30 min at room temperature. The cells were then incubated overnight at 4 °C with the following primary antibodies diluted in Serum-Free Protein Block: CB1R (in 1:50, SC-20754, Santa Cruz, Heidelberg, Germany), RyR (in 1:500, MA3-925, Thermo Fisher Scientific, Waltham, MA, USA), α-actinin (in 1:50, SC-7453, Santa Cruz). Then, Cy3 (in 1:800, A-10520, Thermo Fisher Scientific), Alexa Fluor 488 (in 1:800, A-11001, Thermo Fisher Scientific) and Dylight 488 (in 1:800, DI-3088, Vector Laboratories, Burlingame, CA, USA) labelled secondary antibodies were applied for 1 h at room temperature. Vectashield mounting medium with DAPI (Vector) was used to make the nuclei visible. Images were taken using LSM 510 META confocal microscope (Zeiss, Oberkochen, Germany) with a Plan-Neofluar 40×/1.3 Oil DIC objective (Zeiss). For

statistical analysis of the images, Imaris scientific image processing and analysing software (Bitplane, Zurich, Switzerland) was applied.

2.9. Single-cell calcium imaging

Changes in intracellular calcium concentration ($[Ca^{2+}]_i$) of C2C12 myotubes and isolated FDB fibres were measured using the calcium sensitive fluorescent dye Fura-2 as reported earlier (Oláh et al. 2011). Cells were continuously washed with normal Tyrode's solution using a background perfusion system. Test solutions were directly applied onto the cells through a perfusion capillary tube (Perfusion Pencil™; AutoMate Scientific, San Francisco, CA, USA) with an internal diameter of 250 μm at a 0.35 ml/min rate, using a local perfusion system (Valve Bank™ 8 version 2.0, AutoMate Scientific). Excitation wavelength was alternated between 340 and 380 nm by a dual wavelength monochromator (Deltascan, Photon Technology International, New Brunswick, NJ, USA), while the emission was monitored at 510 nm using an interference filter and a photomultiplier. $[Ca^{2+}]_i$ was calculated from the ratio of fluorescence intensities ($R = F_{340}/F_{380}$) using an *in situ* calibration (Oláh et al. 2011). The Ca^{2+} binding to intracellular binding sites, and the removal of Ca^{2+} from the intracellular space was modelled as presented in earlier reports (Szappanos et al. 2004; Oláh et al. 2011) to determine the activity of the Ca^{2+} pump and the Ca^{2+} flux entering the myoplasmic space.

The CB1R agonists WIN, Arachidonyl-2'-chloroethylamide (ACEA; Cayman Chemical, Tallinn, Estonia) and anandamide (AEA; Tocris) were used at a final concentration of 1 or 10 μM in normal Tyrode's solution. KCl was applied in 120 mM final concentration in normal Tyrode's solution by replacing equal amount of NaCl. ATP was used in a final concentration of 180 μM. 4-chloro-m-cresol (4-CMC), the direct activator of RyR was used in 2 mM. When FDB fibres were measured, 50 μM N-benzyl-P-toluenesulfonamide (Tocris) was added in the solutions to prevent the contraction of the fibres. Pertussis toxin (PTX; from Sigma) was used in 1 μg/ml concentration as an overnight pre-treatment in some experiments.

2.10. Western-blot analysis

Whole hind limb muscle homogenates of at least 3 WT and 3 KO mice were collected separately and Western-blot analysis was performed as described previously (Oláh et al. 2011). For this study, the following antibodies were used: SERCA1 (in 1:1000; a kind gift from E. Zádor), RyR1 (in 1:1000, MA3-925, Thermo Fisher Scientific), DHPR (in 1:500, MA3-921, Thermo Fisher Scientific), FKBP12 (in 1:200, sc-6174, Santa Cruz), calsequestrin (CSQ, in 1:1000, PA1-913, Thermo Fisher Scientific), STIM1 (in 1:500, 610954, BD Biosciences, Franklin Lakes, NJ, USA), Orai1 (in 1:500, MA5-1577, Thermo Fisher Scientific), CB2R (in 1:1000, AB45942, Abcam, Cambridge, UK), PKA (in 1:100, sc-365615, Santa Cruz), and actin (in 1:200, sc-1616 and sc-1616-R, Santa Cruz). As secondary antibodies, horseradish peroxidase conjugated goat anti-mouse and goat anti-rabbit IgGs (1:1000, BioRad) were employed and the immunoreactive bands were visualized by a SuperSignal West Pico or Femto Chemiluminescent Substrate-Enhanced Chemiluminescence kit (Thermo Fisher Scientific) using Gel Logic 1500 Imaging System (Kodak, Tokyo, Japan). Densitometric analysis was performed with ImageJ. Optical density of the bands was normalized to actin of the same sample, then to WT.

2.11. Detection of the changes in $[Ca^{2+}]_i$ using confocal microscopy

Confocal measurements were performed as described earlier (Bodnár et al. 2014). To mimic the conditions used for the force measurements, individual action potentials and tetanic depolarisations were initiated by field-stimulation using supra-threshold single 2 ms long square pulses or trains of 2 ms long square pulses with a frequency of 50 Hz within the train. Each train lasted for 100 ms. Depolarization-evoked calcium transients were measured using a confocal laser scanning microscope system (LSM 5 Live and LSM 510 Meta, Zeiss) after loading the fibres with 20 μM Rhod-2 AM or Fluo-8-AM (Biotium, Inc., Hayward, CA, USA) for 30 minutes at room temperature. Line-scan images (512 pixels/line) were used to monitor the fluorescence intensity changes at 0.5 or 1.93 ms/line and using a 20x/0.5 objective. To obtain the time-course of Rhod-2 fluorescence change, corresponding data points (usually 10-15) in the line-scan images were averaged in the spatial domain. Resting fluorescence was determined as the average fluorescence before the depolarization. Changes in $[Ca^{2+}]_i$, the released amount

of Ca^{2+} ($[Ca^{2+}]_T$), and the calcium release flux were calculated as described in our previous work (Bodnár et al. 2014). 1 μM PKI 14-22 amide, myristoylated (PKI; Tocris), the inhibitor of PKA, and 20 μM gallein (Tocris), the inhibitor of the Gβγ subunit were used as 5 min long treatments between two consecutive single stimulatory impulse-evoked Ca^{2+} transients. The drugs were dissolved in DMSO, and DMSO alone was used as a vehicle control.

2.12. Statistical analysis

Data are presented as mean ± standard error of the mean (SEM) with n as number of observations. Normality of the data was tested with Shapiro-Wilk test. In paired experiments Student's Paired T-test or Wilcoxon Signed Rank Test was used to determine significant differences depending on the normality of the data. When two, non-paired groups were compared, Student's T-test or Mann-Whitney Rank Sum Test was applied. When multiple groups were compared, One Way Analysis of Variance (ANOVA) or Kruskal-Wallis One Way Analysis of Variance on Ranks was used to determine significant differences between the groups, followed by Holm Sidak's or Dunn's multiple comparisons test, respectively. In all tests, differences were considered significant at $p<0.05$. Analyses were performed with SigmaPlot 12.0 (Systat Software, Inc., San Jose, CA, USA), and GraphPad Prism 6 (GraphPad Software, Inc., La Jolla, CA, USA).

3. RESULTS

3.1. CB1 receptors are localized around the Z-lines of adult muscle fibres

Expression of CB1R has been shown in skeletal muscle (Crespillo et al. 2011; Cavuoto et al. 2007); however, its subcellular localization has not been investigated yet. Here, enzymatically isolated *flexor digitorum brevis* (FDB) fibres from wild type (WT) mice were co-immunolabelled with antibodies against CB1R and RyR (Fig 1A-F), and fluorescence intensities of the images on D-F panels were plotted to examine the overlap of red and green signals (Fig 1G-I). RyR showed a typical double-band labelling, corresponding to the localization of two T-tubules in each sarcomere. CB1R showed a striated pattern between the double bands corresponding to the RyR, indicating its localization in the I-band, around the Z-line. The ratio of the co-localizing pixels was 12.4±2.5% (n=11).

To define the localization of CB1Rs more accurately, CB1R and α-actinin were co-immunolabelled (Fig 1G-I), and fluorescence intensities of the images were plotted on J-L panels. The peaks of the fluorescence intensity curves clearly overlapped (Fig 1L), confirming the co-localization of the two proteins at the Z-line. The ratio of the co-localizing pixels was 60.7±10.7% (n=6), which was significantly higher ($p<0.005$) compared to that of CB1R and RyR. The Pearson's correlation coefficients were also determined, the values were 0.065±0.016 for CB1R and RyR, while 0.370±0.047 for CB1R and α-actinin.

3.2. *In vivo* and *in vitro* muscle force and fatigability are altered in CB1R KO and CB1R agonist treated muscles

To examine the effects of CB1 receptor deficiency on *in vivo* muscle performance, activity-wheel tests (Fig 2A-C), wire hang tests (Fig 2D) and forepaw grip tests (Fig 2E) were performed, where CB1R KO (KO) mice performed significantly worse ($p<0.01$) compared to WT. These differences may indicate a deficiency (i) of primary muscular origin or (ii) on the nervous system side. To address the former option in more detail, *in vitro* force measurements were performed.

A series of twitch or tetanic electrical stimulation was applied to isolated *extensor digitorum longus* (EDL; Fig 3) and *soleus* (Sol) muscles, and force was recorded in the

absence or presence of the CB1R agonist WIN55,212-2 (WIN; 1 μM). Neither twitch (Fig 3A, B, E), nor tetanic (Fig 3C, D, F) muscle force of KO mice differed ($p>0.05$) from WTs. WIN seemed to be ineffective both in short series of contractions of whole muscles (Fig 3E-F), and also in small EDL fibre bundles (data not shown), but interestingly, a 1 h treatment of the WT muscles with 1 μM WIN significantly ($p<0.05$) increased fatigability (Fig 3G). Similarly to EDL, we did not observe any significant differences for whole Sol muscles in the force either between WT and KO, or in the absence and presence of WIN (data not shown). Furthermore, a 1 h pre-treatment of WT Sol muscles with 1 μM WIN significantly ($p<0.05$) increased fatigability (data not shown).

To examine the possibility that these changes were due to alterations in the calcium sensitivity of the contractile proteins, pCa-force relations were assessed in untreated and 1 μM WIN-pre-treated and then permeabilized WT fibre bundles (Fig 3H). The normalized pCa-force relationships were fitted with a Hill equation (Fig 3I). The Hill coefficient did not change ($p=0.15$), but the pCa_{50} value was lower ($p<0.05$) in the WIN-treated fibre bundles (Fig 3J), showing that the Ca^{2+} sensitivity of the contractile apparatus significantly decreased when CB1Rs were activated. That is, in WIN-treated fibre bundles a higher elevation of $[Ca^{2+}]_i$ is needed (6.7±0.5 μM *vs*. 5.2±0.4 μM in pre-treated *vs*. untreated, respectively) to achieve the half-maximal activation of the contractile apparatus.

3.3. CB1R agonists do not evoke Ca^{2+} transients via the IP_3 pathway in myotubes and adult muscle fibres

To examine the direct effects of CB1R agonists on the Ca^{2+} homeostasis of skeletal muscle cells in different developmental stages, 1 μM ACEA and 1 μM WIN were administered to Fura-2-loaded terminally differentiated C2C12 myotubes (n=51; Fig 4A) and FDB muscle fibres from WT mice (n=53; Fig 4B). None of these agonists was able to evoke a Ca^{2+} transient, in contrast to the 120 mM KCl and 180 μM ATP used as viability controls. To examine the possibility that peripheral CB1 receptors have lower affinity for the aforementioned agonists, ACEA and WIN were applied in a 10 μM concentration on WT FDB fibres (Fig 4C), but none of the tested fibres (n=13) responded to these agonists with a Ca^{2+} transient in contrast to the 120 mM KCl.

In C2C12 myotubes, the regulatory effects of CB1Rs on the IP_3-mediated Ca^{2+} release were also tested. The IP_3 pathway was activated by 180 μM ATP in Ca^{2+}-free solution (to activate only the P2Y metabotropic without the effects of Ca^{2+} entry via P2X ionotropic purinergic receptors; Burnstock et al. 2013) in the absence (Fig 4D) and presence (Fig 4E) of the CB1R agonist 1 μM WIN. The amplitude of the ATP-evoked Ca^{2+} transients did not differ significantly ($p=0.76$) between untreated and WIN-treated myotubes (Fig 4F).
These observations strongly suggest that CB1 receptors are not coupled functionally to G_q proteins and the IP_3 pathway in skeletal muscle.

3.4. In developing muscle the CB1R agonist WIN has no effect on Ca^{2+} transients

To determine the functionality of CB1 receptors in developing muscle, the effects of the CB1R agonist 1 μM WIN was tested on the KCl depolarization-evoked Ca^{2+} transients of terminally differentiated C2C12 myotubes loaded with Fura-2 (Fig 5). Both in the absence (Fig 5A) and presence of WIN (Fig 5B), the amplitude of the 2nd transient evoked by KCl-depolarization was marginally lower, although statistically significant ($p<0.05$), compared to the 1st one (Fig 5C). The presence of WIN did not alter ($p=0.55$) the amplitude of the 2nd transients compared to the untreated ones. Furthermore, the relation between the amplitudes of the second and first transients – expressed as a percentage of the first transient – was unchanged in the presence of WIN (92±3%, n=14 in untreated *vs*. 91±3%, n=15 in WIN-treated cells; $p=0.72$; Fig 5D). These results indicate that CB1 receptors have no effect on the DHPR-RyR-mediated Ca^{2+} release on cells in the myotube stage of muscle development.

3.5. Depolarization-evoked Ca^{2+} transients are augmented in KO fibres, and can be attenuated by the CB1R agonist WIN and AEA in WT fibres

To explore the function of CB1 receptors in the regulation of depolarization-evoked Ca^{2+} transients in adult muscle, FDB fibres were enzymatically isolated from WT and KO mice. Ca^{2+} release in Fura-2 loaded fibres was activated by repeated application of 120 mM KCl (Fig 6A, B). The amplitude of the 1st Ca^{2+} transients was significantly ($p<0.01$) higher in KO fibres as compared to WT (Fig 6G). Our observation – that the ablation of CB1 receptors causes an increase in the depolarization-evoked Ca^{2+}

transients – suggests a constitutive CB1R activity (Nie and Lewis 2001) and a sustained negative regulatory role of these receptors on ECC which was abolished in the KO animals.

To examine this hypothesis, the effect of 1 μM WIN was studied on KCl-evoked Ca^{2+} transients (Fig 6C, D). Two transients were evoked; the only difference was the absence or presence of WIN after the 1st transients. While the presence of WIN significantly ($p<0.01$) reduced the amplitude of the 2nd KCl-evoked transients in WT fibres, it had no such effect in KO fibres (Fig 6H). In addition, the effect of WIN in WT fibres was greatly occluded by an overnight treatment with 1 μg/ml pertussis toxin (PTX; Fig 6E, H), an inhibitor of $G_{i/o}$ proteins. Similar effect was not observable in PTX treated KO fibres (Fig 6F, H).

To further quantify these results and to enable the comparison between the different groups, the ratio of the amplitudes of the transients was calculated. The ratio is obtained by dividing the amplitude of the second transient by that of the first of the same fibre. This ratio decreased significantly in WT fibres upon WIN treatment (72±5%, n=25 in untreated *vs*. 44±7%, n=27 in WIN-treated fibres; $p<0.01$; Fig 6H), but was similar to the untreated ones in KO fibres (61±4%, n=47 in untreated *vs*. 61±5%, n=27 in WIN-treated fibres; $p=0.98$; Fig 6H). This indicates that WIN not only attenuated the amplitude of the Ca^{2+} transients in WT fibres, but also that this effect was specific for CB1Rs. Moreover, PTX treatment in WT fibres reversed the effect of WIN on this ratio to a value similar to that observed in KO fibres (63±7%, n=18; $p>0.05$; Fig 6H), but was ineffective in KO fibres (62±7%, n=8).

Since WIN is a synthetic agonist of the cannabinoid receptors, the effects of the endogenous CB1R agonist anandamide (AEA) was also tested on WT FDB fibres. The presence of AEA significantly ($p<0.01$) reduced the amplitude of the 2nd KCl-evoked transients. The ratio of the 2nd transient of each cell compared to their 1st transient was smaller in AEA-treated (49±6%, n=14) than in untreated (72±5%, n=25) fibres ($p<0.01$; Fig 6H). These results strengthen the previous observations that CB1 receptors negatively regulate the depolarization-evoked Ca^{2+} release.

3.6. SERCA activity and expression are reduced, while the Ca^{2+} flux via RyRs is increased in KO fibres

The maximal transport rate of the SR Ca^{2+} ATPase (SERCA) pump (PV_{max}) was determined from the declining phase of the Ca^{2+} transients following the KCl-depolarization (Szappanos et al. 2004; Oláh et al. 2011). In KO FDB fibres, PV_{max} was not significantly different ($p=0.06$) from WT; and in WT, but not in KO, it increased significantly after PTX treatment ($p<0.01$) (Fig 7A). On the other hand, WIN treatment did not have any effect on the SERCA pump activity as assessed by comparing PV_{max} values determined from Ca^{2+} transients measured before and after the application of the drug (Fig 7B). A reduced protein expression of SERCA was observed in KO muscles (Fig 7C-D), which was, at first, unexpected as PV_{max} was similar to that in control (Fig 7A). The apparent contradiction can be reconciled in light of the effect of PTX on PV_{max}, which indicates a primary increase in the activity of the individual pumps if the effect of CB1Rs is blocked, followed by a secondary, compensatory reduction in SERCA expression, negating the primary effect. In PTX-treated KO fibres, the PV_{max} of SERCA was similar to that of the untreated KO fibres, and significantly lower than what was observed in PTX-treated WT (Fig 7A). These results suggest that KO fibres lack the constitutive activity of $G_{i/o}$ protein-mediated signalling which was present in the WT, indicating that CB1Rs are the only or the most dominant receptors in adult skeletal muscle having a constitutive $G_{i/o}$ activity.

Other proteins involved in the Ca^{2+} homeostasis of the skeletal muscle, PKA and CB2Rs were also examined, but their expression did not change significantly in KO muscles (Fig 7C-D).

Knowing the PV_{max} values, the maximal Ca^{2+} flux via RyRs was determined (Fig 7E-F). In KO fibres, this parameter was significantly ($p<0.01$) higher than in WT fibres (Fig 7G). In addition, in WT fibres, WIN treatment significantly ($p<0.01$) reduced the flux of the 2^{nd} transients normalized to the 1^{st} ones from 72±4% (n=25) to 46±7% (n=24) (Fig 7H). In KO fibres, WIN treatment did not cause such differences (67±4%, n=46 in untreated, and 70±4%, n=27 in WIN-treated fibres, $p=0.67$) indicating the CB1R-specificity of the effect (Fig 7H). In WT but not in KO, a pre-treatment with PTX rescued the effects of WIN ($p<0.05$), increasing the normalized flux to a comparable value (67±7%, n=18) in untreated WT and KO fibres (Fig 7H).

The effect of WIN on 4-CMC (the direct activator of RyR) evoked Ca^{2+} transients was tested in WT fibres (Fig 7I-J). It did not alter the amplitude (Fig 7K) and the maximal

rate of rise (Fig 7L) of the 4-CMC evoked transients, suggesting that not the agonist-mediated opening of RyR, but its activation via coupling with DHPRs is altered by the CB1R-mediated signalling.

3.7. Tetanic stimulation evokes higher Ca^{2+} transients with increased calcium release flux in KO fibres

To examine the CB1R-mediated effects on the Ca^{2+} transients under physiologically more relevant conditions, confocal line-scan images were recorded in Rhod-2-loaded, field-stimulated FDB fibres of WT (Fig 8A, C) and KO (Fig 8B, D) mice. In KO fibres, tetanic stimuli, but not single pulses, evoked significantly ($p<0.05$) higher Ca^{2+} transients (Fig 8E), in agreement with the findings for the 1st transients by KCl depolarization (Fig 6G). The calculated total amount of calcium released ($[Ca^{2+}]_T$) (Fig 8F-H) and the peak of the calcium release flux through the RyRs (Fig 8I-K) (Bodnár et al. 2014) were similarly higher in KO fibres as compared to WT ($p<0.01$ and $p<0.05$, respectively).

To test whether the direct pharmacological inhibition of PKA has similar effects to its CB1R-mediated, $G_{i/o}$ protein dependent inhibition, 1 μM PKI was applied on WT fibres for 5 min between two consecutive single stimuli. Compared to control fibres, PKI significantly ($p<0.01$) reduced the relative amplitude of the second transients (Fig 8L), similarly to that observed in WIN-treated fibres, supporting the involvement of the $G\alpha_{i/o}$ subunits in the effect. 20 μM gallein, an inhibitor of the Gβγ subunits was also tested on WT fibres, but it did not alter significantly ($p=0.3$) the amplitude of the transients (Fig 8L), suggesting that the involvement of these subunits in the CB1R-mediated regulation of ECC is negligible.

4. DISCUSSION

4.1. CB1R activation causes muscle fatigue

In this study, we describe, to our knowledge for the first time that the cannabinoid receptor mediated signalling also participates in the regulation of ECC and Ca^{2+} homeostasis of mammalian skeletal muscle.

CB1R-KO mice performed significantly worse in all of our *in vivo* muscle performance tests. This was most likely not a direct effect of the lack of CB1Rs in skeletal muscle, rather it was caused by the lack of the receptor in the central nervous system causing depression (Valverde and Torrens 2012) and a reduction in the motivation of the mice to perform exercise. This idea was strengthened by the results of our *in vitro* force measurements, where no significant difference was observed in the twitch and tetanic force of KO, WT and WIN-treated muscles. Our observations also suggest that the neural background, and not the direct effects on the muscles dominated in the medical marijuana-induced muscle weakness of some human patients (Lorente Fernandez et al. 2014) and the cannabinoid-induced hypoactivity of mice (Zimmer et al. 1999) observed by other groups. This forms a contrast to isolated frog muscle fibre bundles, where cannabinoids had substantial direct effects on the muscles themselves (Huerta et al. 2009). For this contrast, probably the physiological differences between amphibian and mammalian muscles were responsible.

On the other hand, we found that the CB1R agonist-treated, isolated WT muscles were significantly more prone to fatigue. This suggests that CB1Rs of the muscles were also, to some extent, directly involved in the marijuana-induced fatigue observed by Renaud and Cormier (1986) in human patients. Cannabinoid-induced fatigue can have several explanations. CB1R agonists were shown to decrease the formation of new mitochondria (Tedesco et al. 2010); however, it is unlikely that this effect could be responsible for such a rapid change (~ 1 hour). CB1R agonists can also decrease respiration in mitochondria by activating mitochondrial CB1Rs (Bénard et al. 2012), therefore reducing ATP production required for sustained muscle exercise. CB1R agonists also decrease the basal and the insulin-mediated glucose uptake (Lindborg et al. 2010), thus, reducing the metabolic supply required for exercise. During our pCa-force measurements, a CB1R-mediated reduction in the Ca^{2+} sensitivity

of the contractile proteins was also observed, i.e. a higher [Ca^{2+}] was needed to achieve the same contractile force in WIN-treated fibres, which might not be able to fully explain, but could contribute to the increased fatigability, especially, as we demonstrated later, that the Ca^{2+} release was also compromised. Thus, next, we examined in detail the role of CB1R-mediated pathways in the Ca^{2+} homeostasis of the developing myotubes and adult fibres.

4.2. CB1 signalling in skeletal muscle does not affect the IP_3 pathway

Activation of CB1Rs was suggested to activate G_q proteins and to release Ca^{2+} from the intracellular stores via IP_3 receptors in a number of different cell types including astrocytes (Navarrete and Araque 2008), dorsal root ganglion neurons (Liu et al. 2009), insulinoma cells (De Petrocellis et al. 2007), and CB1R expressing HEK293 cells (Lauckner et al. 2005). In CB1R expressing CHO cells, the connection of CB1Rs to G_q proteins and phosphatidylinositol 4,5-bisphosphate depletion was also demonstrated, and the same was also proposed for cultured skeletal muscle cells (Iannotti et al. 2014). Here, we tested the highly specific CB1R agonist ACEA and the general CB1R and CB2R agonist WIN on C2C12 myotubes and on adult FDB fibres. Although members of the IP_3 pathway are present on skeletal muscle (Jaimovich et al. 2000), none of these drugs could evoke Ca^{2+} transients, showing that in skeletal muscle – in contrast with heterologous expression systems, neural, or epithelial cells – CB1Rs are not connected to G_q proteins, rather (as will be discussed below) to $G_{i/o}$ proteins as suggested by Huerta et al. (2009), and do not induce a release of Ca^{2+} via IP_3 receptors. Additionally, by examining the effects of CB1R activation on the P2Y metabotropic purinergic receptor-mediated Ca^{2+} transients, we could conclude that the CB1R-mediated signalling does not even regulate the IP_3-mediated Ca^{2+} release in myotubes.

4.3. CB1R attenuates ECC via $G_{i/o}$ proteins

By ruling out coupling to G_q proteins, we assumed that CB1Rs couple to $G_{i/o}$ proteins, and decrease the activity of adenylyl cyclase and protein kinase A (PKA). This then reduces the extent of phosphorylation of different proteins, presumably including DHPR (Hulme et al. 2005; Fuller et al. 2014), RyR (Igami et al. 1999; Ozawa 2010), and regulatory proteins of SERCA (Morita et al. 2008), all of them playing important

roles in ECC. To confirm this hypothesis, the effects of the absence and the activation of CB1Rs was studied on depolarization-evoked Ca^{2+} transients.

Interestingly, in C2C12 myotubes, we could not detect any effects of CB1R activation, indicating that some components of the CB1R-mediated signalling pathway are not yet present or functional on these cells. Or at this stage of muscle development, CB1R activation only affects myogenesis (Iannotti et al. 2014), without influencing the Ca^{2+} signalling mechanisms.

On the other hand, in adult KO skeletal muscle fibres, the absence of CB1Rs significantly increased the amplitude of the depolarization-induced Ca^{2+} transients, the total amount of Ca^{2+} released during tetanic stimulation, and the Ca^{2+} release flux through RyR. These indicate RyR as one of the possible main downstream targets of the CB1R mediated signalling, and also suggest the presence of a continuous negative control on these Ca^{2+} release channels mediated by a CB1R dependent pathway in WT muscles. The above mentioned inhibitory effect was further amplified by activation of CB1Rs by WIN or AEA in WT but not in KO fibres proving the CB1R-specificity of this phenomenon.

At a first glance, there seems to be a contradiction between the higher Ca^{2+} but similar force transients in KO muscles as compared to WT. However, in the case of tetani, we can assume that the relatively smaller amplitude of the Ca^{2+} transients in WT (even in WIN-treated WT) is already capable of fully activating the contractile system. In this framework two conclusions follow. First, in a normal (WT) muscle the tetanic stimulation fully activates the contractile machinery (there is no need to have any reserve; this is done by not activating all fibres in the given muscle), therefore larger force transients are not expected even if $[Ca^{2+}]_i$ is greater. Second, any further increase in released Ca^{2+} is a “waste”, and does not generate larger force. In this respect CB1R mediated signalling helps muscles to be more “efficient”. One could take this speculation even further by stating that if, for any reason, the function of the contractile machinery is altered, there is a reserve in the system (“turning off” the constitutive activity of the cannabinoid signalling) to improve/increase force.

The effect of the CB1R agonist treatment was reversible by inhibiting $G_{i/o}$ proteins with pertussis toxin, confirming the involvement of these G proteins in the CB1R mediated signalling. Moreover, the direct pharmacological inhibition of PKA

resulted in a similar effect, i.e. a marked reduction of the Ca^{2+} transients, strengthening the conclusions drawn from our previous experiments. Thus, it can be proposed that in adult skeletal muscle fibres the agonist-mediated or constitutive (Nie and Lewis 2001) activity of CB1R activates $G_{i/o}$ proteins, which decreases the level of cAMP, the activity of PKA, and the phosphorylation of RyR (Igami et al. 1999; Ozawa 2010) or other proteins involved in ECC (e.g. the DHPR), thereby decreasing the magnitude of the RyR-mediated Ca^{2+} current (Fig 9). However, an indirect regulatory effect of the CB1R-mediated signalling on SR Ca^{2+} release, where the recovery from inactivation of the above mentioned receptors is affected, cannot be ruled out either.

Although several research groups demonstrated that cannabinoids inhibit other (N, P, P/Q, and T) types of Ca^{2+} channels (for review see e.g. Pertwee et al. 2010), and Zhuang et al. (2005) described the regulatory effect of these drugs on RyRs in hippocampal neurons, yet in muscle, to our knowledge, the present study is the first to demonstrate any role of the cannabinoid system in the RyR mediated Ca^{2+} release and ECC. In skeletal muscle, the localization of CB1Rs around the Z-lines, between the T-tubules of the muscle fibres also supports the idea of an effective, spatially coordinated regulatory apparatus with the involvement of both receptors. If RyRs are regulated by CB1Rs similarly in amphibians, our results can explain those previous observations where CB1R-agonist treatment caused weaker contractile force of frog muscles (Huerta et al. 2009). Moreover, they resemble to the results obtained on smooth (Baldassano et al. 2008; Makwana et al. 2010; Grassin-Delyle et al. 2014; Sánchez-Pastor et al. 2014) and cardiac muscle (Bonz et al. 2003; Li et al. 2009), where CB1R agonists similarly attenuated and the antagonists enhanced muscle contractions and Ca^{2+} transients, although in none of these studies were RyRs mentioned among the downstream targets of cannabinoid signalling.

Our experiments with 4-CMC, the direct activator of RyR suggest that the DHPR-RyR interaction is affected by the cannabinoid signalling, and not the Ca^{2+} release via agonist-mediated opening of RyR. However, these experiments do not discriminate whether the CB1R mediated effects take place at the RyR's or DHPR's side in ECC. Thus, we cannot rule out the effects of PKA-phosphorylation of DHPRs in the increased Ca^{2+} transients of the KO fibres. PKA is anchored by an A-kinase anchoring protein to the autoinhibitory distal C terminus of the skeletal and cardiac

voltage-gated Ca^{2+} channels (CaV1). Protein phosphorylation by PKA increases ion conductance activity by relieving the autoinhibitory effect of the distal C terminus (Hulme et al. 2005, Fuller et al. 2014), but it is not known how it affects the voltage sensitivity of DHPR or its conformation change by which RyR is activated during ECC.

It was also conceivable that the effects observed upon CB1R stimulation were not only caused by the activation of the α subunits of the G proteins, but were also mediated to some extent by their Gβγ subunits. Activation of G protein coupled receptors following extracellular agonist stimulation results in the activation of two intracellular signalling molecules, Gα-GTP (its presumable effects were discussed above in detail) and the free Gβγ dimer. Gβγ-mediated regulation generally occurs through direct binding of the dimer to target effectors. In neurons, the Gβγ dimer is known to inhibit CaV through its direct binding to the CaV2 α subunit (for review, see e.g. De Waard et al. 2005). A relatively recent study in adult mammalian skeletal muscle has shown that the expression of Gβ1γ2 dimer inhibits the CaV1.1 (DHPR) Ca^{2+} current and the voltage-activated SR Ca^{2+} release process (Weiss et al. 2010). Thus, it was possible that the observed regulatory effects on ECC were not exclusively arising from CB1R dependent activation of $G\alpha_{i/o}$, but instead due to CB1R dependent regulation of CaV1.1 (or indirect regulation of RyR1) mediated by Gβγ subunits. In support of this view, CB1R activation is associated to Gβγ-dependent activation of different effectors including ion channels, the kinases PI3K, Src, and MAPK cascades (Keimpema et al. 2011). In addition, CB1R signals also through non-G protein partners such as the adaptor protein FAN (factor associated with neutral sphingomyelinase activation). However, inhibition of the Gβγ subunits did not alter the amplitude of the Ca^{2+} transients significantly, suggesting that the role of these subunits in the CB1R-mediated regulation of ECC is negligible in skeletal muscle.

4.4. CB1R attenuates SERCA activity

A CB1R mediated decrease in the PKA activity may also affect the regulatory proteins of the SERCA pump: phospholamban (PLB) in slow skeletal muscle and heart (Liu et al. 1997), and sarcolipin (SLN) in fast skeletal muscle (Odermatt et al. 1998). PKA-mediated phosphorylation of PLB and SLN leads to their conformational change,

and to a higher Ca^{2+} uptake rate of SERCA (Morita et al. 2008), thus, CB1R activation was expected to reduce SERCA activity.

Consistently with this, in PTX-treated WT fibres, as a result of the enhanced PKA activity, a markedly increased Ca^{2+} transport rate was observed. In KO fibres, where we also expected a higher PKA and SERCA activity due to the missing constitutive inhibitory action of CB1Rs and the coupling $G_{i/o}$ proteins, surprisingly, the PV_{max} was similar to that of the untreated WT. Taking into consideration the significantly reduced SERCA expression of KO muscles, and as the total PV_{max} was found to be similar to that of WT, the individual pump activity, in fact, had to be significantly higher in KO fibres. This means that the increased pump activity in KO fibres was masked by a compensatory reduction in the SERCA protein expression. Thus, similarly to the case of RyR, we can assume a continuous negative regulatory effect of the CB1R mediated signalling on SERCA activity in WT fibres, which was missing in KO fibres.

On the other hand, SERCA activity was not affected by WIN treatment, suggesting that PLB/SLN are normally dephosphorylated in WT fibres, and their phosphorylation state could not be further decreased by the activation of the CB1R-mediated signalling.

It is worth noting that the expression of the main Ca^{2+} binding protein of the SR Ca^{2+} store – calsequestrin– was mostly unchanged in KO muscles. Likewise, the expression of stromal interaction molecule 1 (STIM1), the Ca^{2+} sensor of the SR, and key activator molecule of the store-operated Ca^{2+} entry (SOCE) mechanism, and Orai1, the main store-operated Ca^{2+} channel (Pan et al. 2014) was also unaltered in KO muscles. According to the PhosphoSitePlus® database (Hornbeck et al. 2015), these proteins are not phosphorylated by PKA. These observations suggest that CB1R-mediated signalling most probably does not interfere with Ca^{2+} storage functions of the SR. In CB2R expression, we also did not find any difference between WT and KO muscle samples, ruling out the possibility that the lack of CB1R upregulates this other cannabinoid signalling pathway.

4.5. Final conclusions

In summary, the present study provides answers for previously unresolved questions, namely, which signal transduction pathway is connected to CB1Rs in mammalian skeletal muscle, and how the absence or activation of the receptors affects ECC and muscle force. Our results prove that CB1R-mediated signalling in skeletal muscle inhibits the RyR-mediated Ca^{2+} transients via a $G_{i/o}$ protein and PKA dependent way, alters the activity of SERCA, reduces the Ca^{2+}-sensitivity of the contractile proteins, and increases muscle fatigue.

These, together with the results of other research groups – the decrease of myogenesis and myoblast differentiation (Iannotti et al. 2014), the reduction of the glucose uptake of the muscles (Lindborg et al. 2010), the reduction of the mitochondrial biogenesis (Tedesco et al. 2010) and ATP production (Bénard et al. 2012, Fišar et al. 2014), and neuronal effects to decrease the locomotor activity (Zimmer et al. 1999) – point to a complex, systemic inhibitory role of the cannabinoid system on muscle activity. But the same observations raise the possibility that antagonists of CB1Rs could be used as potent stimulators of muscle force and regeneration during aging and in muscle-wasting diseases. These results can contribute to the understanding of the role of the endocannabinoid system in myopathies and the development of new cannabinoid drugs by identifying their muscle-specific action or side-effects, and also call attention to the risks of marijuana smoking on physical performance.

ADDITIONAL INFORMATION

COMPETING INTERESTS

The authors confirm no conflicts of interest.

AUTHOR CONTRIBUTIONS

T.O., D.B., J.V., A.T., J.F., B.R., A.K., O.R., B.D., and P.Sz. performed experiments, and collected, analysed and interpreted data. T.O., O.F. and L.Cs. designed and supervised the study, analysed and interpreted data and wrote the paper. All authors approved the final version of the manuscript. All persons designated as authors qualify for authorship, and all those who qualify for authorship are listed. Measurements of muscle force in small fibre bundles were performed at the Friedrich-Alexander-University Erlangen-Nürnberg. All other experiments were performed at the University of Debrecen.

FUNDING

T.O. and J.V. was supported by the European Union and the State of Hungary, co-financed by the European Social Fund in the framework of TÁMOP 4.2.4. A/2-11-1-2012-0001 'National Excellence Program'. The work was supported by research grants from the Hungarian Scientific Research Fund (OTKA NN-107765), and TÁMOP-4.1.2.E-13/1/KONV-2013-0010.

ACKNOWLEDGEMENTS

The authors are indebted to Róza Őri and Sabine Lessig for their excellent technical assistance, Csilla Bordás, Bíborka Nádró and Anna Farkas for their help in *in vivo* tests and genotyping. CB1R-KO mice were a kind gift from Dr. Andreas Zimmer.

REFERENCES

Baldassano S, Serio R & Mule' F (2008). Cannabinoid CB(1) receptor activation modulates spontaneous contractile activity in mouse ileal longitudinal muscle. Eur J Pharmacol 582, 132-8.

Bénard G, Massa F, Puente N, Lourenço J, Bellocchio,L, Soria-Gómez E, Matias I, Delamarre A, Metna-Laurent M, Cannich A, Hebert-Chatelain E, Mulle C, Ortega-Gutiérrez S, Martín-Fontecha M, Klugmann M, Guggenhuber S, Lutz B, Gertsch J, Chaouloff F, López-Rodríguez ML, Grandes P, Rossignol R & Marsicano G (2012). Mitochondrial CB_1 receptors regulate neuronal energy metabolism. Nat Neurosci 15, 558-64

Bodnár D, Geyer N, Ruzsnavszky O, Oláh T, Hegyi B, Sztretye M, Fodor J, Dienes B, Balogh Á, Papp Z, Szabó L, Müller G, Csernoch L & Szentesi P (2014). Hypermuscular mice with mutation in the myostatin gene display altered calcium signalling. J Physiol 592, 1353-65

Bonz A, Laser M, Küllmer S, Kniesch S, Babin-Ebell J, Popp V, Ertl G & Wagner JA (2003). Cannabinoids acting on CB1 receptors decrease contractile performance in human atrial muscle. J Cardiovasc Pharmacol 41, 657-64.

Borgelt LM, Franson KL, Nussbaum AM & Wang GS (2013). The pharmacologic and clinical effects of medical cannabis. Pharmacotherapy 33, 195-209.

Buckman JF, Yusko DA, Farris SG, White HR & Pandina RJ (2011). Risk of marijuana use in male and female college student athletes and nonathletes. J Stud Alcohol Drugs 72, 586-91.

Burnstock G, Arnett TR & Orriss IR (2013). Purinergic signalling in the musculoskeletal system. Purinergic Signal 9, 541-72.

Cavuoto P, McAinch AJ, Hatzinikolas G, Janovská A, Game P & Wittert GA (2007). The expression of receptors for endocannabinoids in human and rodent skeletal muscle. Biochem Biophys Res Commun 364, 105-10.

Crespillo A, Suárez J, Bermúdez-Silva FJ, Rivera P, Vida M, Alonso M, Palomino A, Lucena MA, Serrano A, Pérez-Martín M, Macias M, Fernández-Llébrez P & Rodríguez de Fonseca F (2011). Expression of the cannabinoid system in muscle: effects of a high-fat diet and CB1 receptor blockade. Biochem J 433, 175-85.

De Petrocellis L, Marini P, Matias I, Moriello AS, Starowicz K, Cristino L, Nigam S & Di Marzo V (2007). Mechanisms for the coupling of cannabinoid receptors to intracellular calcium mobilization in rat insulinoma beta-cells. Exp Cell Res 313, 2993-3004.

De Waard M, Hering J, Weiss N & Feltz A (2005). How do G proteins directly control neuronal Ca2+ channel function? Trends Pharmacol Sci. 26, 427-36.

Devane WA, Hanus L, Breuer A, Pertwee RG, Stevenson LA, Griffin G, Gibson D, Mandelbaum A, Etinger A & Mechoulam R (1992). Isolation and structure of a brain constituent that binds to the cannabinoid receptor. Science. 258. 1946-9.

Esposito I, Proto MC, Gazzerro P, Laezza C, Miele C, Alberobello AT, D'Esposito V, Beguinot F, Formisano P & Bifulco M (2008). The cannabinoid CB1 receptor antagonist rimonabant stimulates 2-deoxyglucose uptake in skeletal muscle cells by regulating the expression of phosphatidylinositol-3-kinase. Mol Pharmacol 74, 1678-86.

Fišar Z, Singh N & Hroudová J (2014). Cannabinoid-induced changes in respiration of brain mitochondria. Toxicol Lett 231, 62-71.

Franzini-Armstrong C & Protasi F (1997). Ryanodine receptors of striated muscles: a complex channel capable of multiple interactions. Physiol Rev. 77. 699-729.

Friedrich O, Yi B, Edwards JN, Reischl B, Wirth-Hücking A, Buttgereit A, Lang R, Weber C, Polyak F, Liu I, von Wegner F, Cully TR, Lee A, Most P & Völkers M (2014). IL-1α reversibly inhibits skeletal muscle ryanodine receptor. a novel mechanism for critical illness myopathy? Am J Respir Cell Mol Biol 50, 1096-106.

Fuller MD, Fu Y, Scheuer T & Catterall WA (2014). Differential regulation of CaV1.2 channels by cAMP-dependent protein kinase bound to A-kinase anchoring proteins 15 and 79/150. J Gen Physiol 143, 315-24.

Grassin-Delyle S, Naline E, Buenestado A, Faisy C, Alvarez JC, Salvator H, Abrial C, Advenier C, Zemoura L & Devillier P (2014). Cannabinoids inhibit cholinergic contraction in human airways through prejunctional CB1 receptors. Br J Pharmacol 171, 2767-77.

Hornbeck PV, Zhang B, Murray B, Kornhauser JM, Latham V & Skrzypek E (2015). PhosphoSitePlus, 2014: mutations, PTMs and recalibrations. Nucleic Acids Res 43(Database issue), D512-20.

Huerta M, Ortiz-Mesina M, Trujillo X, Sánchez-Pastor E, Vásquez C, Castro E, Velasco R, Montoya-Pérez R & Onetti C (2009). Effects of cannabinoids on caffeine contractures in slow and fast skeletal muscle fibers of the frog. J Membr Biol 229, 91-9.

Hulme JT, Konoki K, Lin TW, Gritsenko MA, Camp DG 2nd, Bigelow DJ & Catterall WA (2005). Sites of proteolytic processing and noncovalent association of the distal C-terminal domain of CaV1.1 channels in skeletal muscle. Proc Natl Acad Sci U S A 102, 5274-9

Hutchins-Wiese HL, Li Y, Hannon K & Watkins BA (2012). Hind limb suspension and long-chain omega-3 PUFA increase mRNA endocannabinoid system levels in skeletal muscle. J Nutr Biochem 23, 986-93.

Iannotti FA, Silvestri C, Mazzarella E, Martella A, Calvigioni D, Piscitelli F, Ambrosino P, Petrosino S, Czifra G, Bíró T, Harkany T, Taglialatela M & Di Marzo V (2014). The endocannabinoid 2-AG controls skeletal muscle cell differentiation via CB1 receptor-dependent inhibition of Kv7 channels. Proc Natl Acad Sci U S A 111, E2472-81.

Igami K, Yamaguchi N & Kasai M (1999). Regulation of depolarization-induced calcium release from skeletal muscle triads by cyclic AMP-dependent protein kinase. Jpn J Physiol 49, 81-7.

Jaimovich E, Reyes R, Liberona JL & Powell JA (2000). IP(3) receptors, IP(3) transients, and nucleus-associated Ca(2+) signals in cultured skeletal muscle. Am J Physiol Cell Physiol 278, C998-C1010

Keimpema E, Mackie K & Harkany T (2011). Molecular model of cannabis sensitivity in developing neuronal circuits. Trends Pharmacol Sci. 32, 551-61.

Lauckner JE, Hille B & Mackie K (2005). The cannabinoid agonist WIN55,212-2 increases intracellular calcium via CB1 receptor coupling to Gq/11 G proteins. Proc Natl Acad Sci U S A 102, 19144-9.

Li Q, Ma HJ, Zhang H, Qi Z, Guan Y & Zhang Y (2009). Electrophysiological effects of anandamide on rat myocardium. Br J Pharmacol 158, 2022-9.

Lindborg KA, Teachey MK, Jacob S & Henriksen EJ (2010). Effects of in vitro antagonism of endocannabinoid-1 receptors on the glucose transport system in normal and insulin-resistant rat skeletal muscle. Diabetes Obes Metab 12, 722-30.

Lipina C, Stretton C, Hastings S, Hundal JS, Mackie K, Irving AJ & Hundal HS (2010). Regulation of MAP kinase-directed mitogenic and protein kinase B-mediated signaling by cannabinoid receptor type 1 in skeletal muscle cells. Diabetes 59, 375-85.

Liu Q, Bhat M, Bowen WD & Cheng J (2009). Signaling pathways from cannabinoid receptor-1 activation to inhibition of N-methyl-D-aspartic acid mediated calcium influx and neurotoxicity in dorsal root ganglion neurons. J Pharmacol Exp Ther 331, 1062-70.

Liu Y, Kranias EG & Schneider MF (1997). Regulation of Ca2+ handling by phosphorylation status in mouse fast- and slow-twitch skeletal muscle fibers. Am J Physiol 273, C1915-24.

Lorente Fernández L, Monte Boquet E, Pérez-Miralles F, Gil Gómez I, Escutia Roig M, Boscá Blasco I, Poveda Andrés JL & Casanova-Estruch B (2014). Clinical experiences with cannabinoids in spasticity management in multiple sclerosis. Neurologia 29, 257-60.

Maccarrone M, Bab I, Bíró T, Cabral GA, Dey SK, Di Marzo V, Konje JC, Kunos G, Mechoulam R, Pacher P, Sharkey KA & Zimmer A (2015). Endocannabinoid signaling at the periphery: 50 years after THC. Trends Pharmacol Sci 36, 277-296.

Makwana R, Molleman A & Parsons ME (2010). Evidence for both inverse agonism at the cannabinoid CB1 receptor and the lack of an endogenous cannabinoid tone in the rat and guinea-pig isolated ileum myenteric plexus-longitudinal muscle preparation. Br J Pharmacol 160, 615-26.

Morita T, Hussain D, Asahi M, Tsuda T, Kurzydlowski K, Toyoshima C & Maclennan DH (2008). Interaction sites among phospholamban, sarcolipin, and the sarco(endo)plasmic reticulum Ca(2+)-ATPase. Biochem Biophys Res Commun 369, 188-94.

Navarrete M & Araque A (2008). Endocannabinoids mediate neuron-astrocyte communication. Neuron 57, 883-93.

Nie J & Lewis DL (2001). Structural domains of the CB1 cannabinoid receptor that contribute to constitutive activity and G-protein sequestration. J Neurosci. 21, 8758-64.

Oddoux S, Brocard J, Schweitzer A, Szentesi P, Giannesini B, Brocard J, Fauré J, Pernet-Gallay K, Bendahan D, Lunardi J, Csernoch L & Marty I (2009). Triadin deletion induces impaired skeletal muscle function. J Biol Chem 284, 34918-29.

Odermatt A, Becker S, Khanna VK, Kurzydlowski K, Leisner E, Pette D & MacLennan DH (1998). Sarcolipin regulates the activity of SERCA1, the fast-twitch skeletal muscle sarcoplasmic reticulum Ca2+-ATPase. J Biol Chem 273, 12360-9.

Oláh T, Fodor J, Ruzsnavszky O, Vincze J, Berbey C, Allard B & Csernoch L (2011). Overexpression of transient receptor potential canonical type 1 (TRPC1) alters both store operated calcium entry and depolarization-evoked calcium signals in C2C12 cells. Cell Calcium 49, 415-25.

Ozawa T (2010). Modulation of ryanodine receptor Ca2+ channels (Review). Mol Med Rep 3, 199-204.

Pacher P & Kunos G (2013). Modulating the endocannabinoid system in human health and disease--successes and failures. FEBS J 280, 1918-43.

Pan Z, Brotto M & Ma J (2014). Store-operated Ca2+ entry in muscle physiology and diseases. BMB Rep 47, 69-79.

Pertwee RG, Howlett AC, Abood ME, Alexander SP, Di Marzo V, Elphick MR, Greasley PJ, Hansen HS, Kunos G, Mackie K, Mechoulam R & Ross RA (2010). International Union of Basic and Clinical Pharmacology. LXXIX. Cannabinoid receptors and their ligands: beyond CB_1 and CB_2. Pharmacol Rev 62, 588-631.

Renaud AM & Cormier Y (1986). Acute effects of marihuana smoking on maximal exercise performance. Med Sci Sports Exerc 18, 685-9.

Rowland LA, Bal NC & Periasamy M (2015). The role of skeletal-muscle-based thermogenic mechanisms in vertebrate endotherm. Biol Rev Camb Philos Soc. 90. 1279-97.

Sánchez-Pastor E, Andrade F, Sánchez-Pastor JM, Elizalde A, Huerta M, Virgen-Ortiz A, Trujillo X & Rodríguez-Hernández A (2014). Cannabinoid receptor type 1 activation by arachidonylcyclopropylamide in rat aortic rings causes vasorelaxation involving calcium-activated potassium channel subunit alpha-1 and calcium channel, voltage-dependent, L type, alpha 1C subunit. Eur J Pharmacol 729, 100-6.

Sinacore DR & Gulve EA (1993). The role of skeletal muscle in glucose transport, glucose homeostasis, and insulin resistance: implications for physical therapy. Phys Ther. 73, 878-91.

Stammers AN, Susser SE, Hamm NC, Hlynsky MW, Kimber DE, Kehler DS & Duhamel TA (2015). The regulation of sarco(endo)plasmic reticulum calcium-ATPases (SERCA). Can J Physiol Pharmacol. 93, 843-54.

Szappanos H, Cseri J, Deli T, Kovács L & Csernoch L (2004). Determination of depolarisation- and agonist-evoked calcium fluxes on skeletal muscle cells in primary culture. J Biochem Biophys Methods 59, 89-101.

Taube A, Eckardt K & Eckel J (2009). Role of lipid-derived mediators in skeletal muscle insulin resistance. Am J Physiol Endocrinol Metab 297, E1004-12

Tedesco L, Valerio A, Dossena M, Cardile A, Ragni M, Pagano C, Pagotto U, Carruba MO, Vettor R & Nisoli E (2010). Cannabinoid receptor stimulation impairs mitochondrial biogenesis in mouse white adipose tissue, muscle, and liver: the role of eNOS, p38 MAPK, and AMPK pathways. Diabetes 59, 2826-36.

Turu G & Hunyady L (2010). Signal transduction of the CB1 cannabinoid receptor. J Mol Endocrinol 44, 75-85.

Valverde O & Torrens M (2012). CB1 receptor-deficient mice as a model for depression. Neuroscience 204, 193-206.

Weiss N, Legrand C, Pouvreau S, Bichraoui H, Allard B, Zamponi GW, De Waard M & Jacquemond V (2010). In vivo expression of G-protein beta1gamma2 dimer in adult mouse skeletal muscle alters L-type calcium current and excitation-contraction coupling. J Physiol. 588, 2945-60.

Zhuang SY, Bridges D, Grigorenko E, McCloud S, Boon A, Hampson RE & Deadwyler SA (2005). Cannabinoids produce neuroprotection by reducing intracellular calcium release from ryanodine-sensitive stores. Neuropharmacology 48, 1086-96.

Zimmer A, Zimmer AM, Hohmann AG, Herkenham M & Bonner TI (1999). Increased mortality, hypoactivity, and hypoalgesia in cannabinoid CB1 receptor knockout mice. Proc Natl Acad Sci U S A 96, 5780-5.

FIGURE LEGENDS

Fig. 1

CB1 receptor localizes around the Z-lines of *flexor digitorum brevis* (FDB) fibres. Representative confocal immunofluorescence images showing the localization of **(A, G)** CB1R (labelled with Cy3, red) around the Z-lines, **(B)** ryanodine receptors (RyR, labelled with Alexa Fluor 488, green) in the T-tubules of the SR, and **(H)** α-actinin at the Z-lines (labelled with Dylight 488, green). **(C, I)** Merged images of panels **A-B** and **G-H**, respectively. In the inset of panel **C** and **I** a negative control image is shown, stained with both secondary antibodies and labelling of the nuclei (DAPI, blue). **(D-F,** and **J-L)** Fluorescence intensity of panels **A-C** and **G-I**, respectively, was plotted under each image. Images were recorded from 1 μm thick optical slices. Original magnification was 40×.

Fig. 2

***In vivo* muscle performance of CB1R-KO (KO) and wild type (WT) mice**. **(A)** Average speed, **(B)** maximum speed, and **(C)** average distance per day measured with voluntary activity-wheel test. **(D)** Averaged duration, measured with wire hang tests. **(E)** Averaged maximal force of the animals measured with grip tests. **: $p<0.01$, WT vs. KO mice.

Fig. 3

CB1R activation enhances fatigue and attenuates Ca^{2+} sensitivity. To evoke contractions, repeated series of electrical stimulation were applied to isolated whole *extensor digitorum longus* (EDL) muscles in the absence and presence of the CB1R agonist 1 μM WIN55,212-2 (WIN), and force was measured. **(A, B)** Representative single twitches and **(C, D)** tetani of a **(A, C)** WT and a **(B, D)** KO EDL muscle. Solid line indicates a representative contraction in the absence, while dashed line indicates one in the presence of WIN. Pooled data of the amplitudes of **(E)** single twitches and **(F)** tetani in the absence and presence of WIN. Numbers in parentheses show the number of muscles studied.

(G) Time course of the amplitude of tetani in EDL muscles. Altogether, 150 tetani, repeated every 2 s, were evoked, and their amplitudes normalized to the maximum train value. Measurements were pooled from 6 KO, 6 WT, and 5 WIN-treated (1 μM for 1 hour) WT EDL muscles. §: $p<0.05$, WIN-treated vs. untreated muscles.
(H) Representative pCa–relative force curves of an untreated and a 1 μM WIN-pre-treated WT EDL fibre bundle. Numbers on arrows indicate the pCa steps. **(I)** Hill-fit of the pCa-force values normalized to the maximal force. **(J)** Pooled data of Hill coefficients and pCa_{50} values. (n): number of fibre bundles. §: $p<0.05$, WIN-treated *vs*. untreated fibre bundles.

Fig. 4

CB1R agonists do not evoke Ca^{2+} transients via the IP_3 pathway in myotubes and adult muscle fibres. Representative traces of single-cell $[Ca^{2+}]_i$ measurements performed on Fura-2-loaded **(A)** C2C12 myotubes (n=51) and **(B)** *flexor digitorum brevis* (FDB) fibres of WT mice (n=53). The CB1R agonists 1 μM arachidonyl-2'-chloroethylamide (ACEA) and 1 μM WIN did not evoke Ca^{2+} transients as opposed to 120 mM KCl or 180 μM ATP used as viability controls. Even when applied at 10 μM **(C)**, these agonists could not evoke Ca^{2+} transients as opposed to KCl in FDB fibres (n=13). However, IP_3 pathway was clearly activated in C2C12 myotubes by administering 180 μM ATP in Ca^{2+}-free Tyrode's solution **(D)** in the absence and **(E)** in the presence of 1 μM WIN. **(F)** Pooled data of the amplitude of the ATP-evoked transients.

Fig. 5

CB1R activation has no effect on the Ca^{2+} transients in myotubes. Representative records showing repeated KCl-depolarization-evoked Ca^{2+} transients of Fura-2 loaded, terminally differentiated C2C12 myotubes. The cannabinoid agonist WIN (1 μM) was **(A)** absent or **(B)** present in the media after the first transient. Pooled data of **(C)** the amplitude of the transients and **(D)** the relationship between the amplitudes of the first and second transients expressed in percentage of the first transient. #: $p<0.05$, first *vs*. second transient of the same cell.

Fig. 6

CB1R activation attenuates; its absence enhances the Ca^{2+} transients in adult FDB fibres via a $G_{i/o}$-mediated way. Repeated KCl-depolarization-evoked Ca^{2+} transients of Fura-2 loaded FDB muscle fibres from KO and WT mice in the absence and presence of CB1R agonists. Representative records of **(A)** a WT and **(B)** a KO FDB fibre in the absence of WIN (1μM). Representative records of **(C)** a WT and **(D)** a KO FDB fibre in the presence of WIN. WIN was continuously applied after the first transients. Representative records of a **(E)** WT and a **(F)** KO FDB fibre pre-treated with 1 μg/ml pertussis toxin (PTX; a $G_{i/o}$ protein inhibitor) overnight before measurement. **(G)** Pooled data of the amplitude of the first transients without PTX. **(H)** The relationship between the amplitudes of the first and second transients expressed in percentage of the first transient. * and **: $p<0.05$ and $p<0.01$, respectively, WT *vs*. KO mice. ##: $p<0.01$, first *vs*. second transient of the same fibre. §§: $p<0.01$, WIN or anandamide (AEA)-treated *vs*. untreated fibres.

Fig. 7

SERCA pump activity and calcium flux in WT, PTX-pre-treated (1 μg/ml, overnight) WT, and KO FDB fibres. Pooled data of **(A)** the calculated transport maximum of the SERCA pumps, and **(B)** the same parameter of untreated and WIN-treated KCl-evoked second Ca^{2+} transients normalized to that of the untreated first transients. **(C)** Representative images of Western-blot experiments showing the expression of proteins involved in the Ca^{2+} homeostasis of skeletal muscle. Whole hind limb muscle homogenates from at least 3 WT and 3 KO mice were used as samples. Spleen of a WT mouse was used as a positive control for CB2R. **(D)** Average optical density of the Western-blot bands normalized to actin and then to WT. Representative records of maximum calcium flux (the amount of calcium entering the cytosol in one second) of KCl-evoked Ca^{2+} transients before and after WIN-treatment in **(E)** WT and **(F)** KO FDB fibres. **(G)** Pooled data of maximum Ca^{2+} flux entering the cytoplasm via RyRs during the first KCl-depolarization of WT and KO FDB fibres. **(H)** relative Ca^{2+} flux normalized to the first transient in untreated and WIN-treated FDB fibres. Repeated 4-CMC-evoked Ca^{2+} transients of WT FDB muscle fibres in the **(I)** absence and **(J)**

presence of WIN. The relationship between **(K)** the amplitudes and **(L)** the slopes of the first and second transients expressed in percentage of the first transient.
Abbreviations not in the list: CSQ: calsequestrin; STIM1L/S: long/short isoform of stromal interaction molecule type 1. * and **: $p<0.05$ and $p<0.01$, respectively, WT vs. KO mice. & and &&: $p<0.05$ and $p<0.01$, respectively, PTX-treated *vs*. untreated WT fibres. §§: $p<0.01$, WIN-treated *vs*. untreated fibres.

Fig. 8

Tetanic electric stimulus evoked Ca^{2+} transients, Ca^{2+} release flux, and amount of released Ca^{2+} are higher in KO fibres. Confocal line-scan images were recorded on Rhod-2-loaded FDB fibres of WT and KO mice during field-stimulation. Representative records of Ca^{2+} transients evoked by a single stimulatory impulse (**A** in WT and **B** in KO FDB) or a tetanic stimulus (**C** in WT and **D** in KO FDB). Time courses were calculated from the average of 8-20 lines marked by arrows on the line-scan images. **(E)** pooled data of the amplitude of the transients. Representative records of the total released amount of Ca^{2+} ($[Ca^{2+}]_T$) in a **(F)** WT and a **(G)** KO FDB fibre. **(H)** Pooled data of $[Ca^{2+}]_T$. (**I** and **J**) the corresponding calcium release flux through RyRs in WT and KO fibres, respectively. **(K)** Pooled data of the peak (1^{st} peak) and steady level (5^{th} peak) of the calcium release flux. **(L)** Two consecutive single stimuli were applied with 5 min delay, and during the intermittent period either PKI (1 μM) or gallein (20 μM) was applied on the fibres. Relative amplitude of the second transients, expressed as the percentage of the first transient on the same fibre before the treatment. Numbers in parentheses show the number of FDB fibres examined. * and **: $p<0.05$ and $p<0.01$, respectively, WT *vs*. KO mice. §§: $p<0.01$, PKI or gallein treated WT *vs.* untreated.

Fig. 9

The proposed mechanism how CB1 receptors regulate excitation-contraction coupling in skeletal muscle. The depolarization of the membrane activates DHPRs which directly open RyRs and release Ca^{2+} from the SR, activating the contractile apparatus of the muscle fibre. The Ca^{2+} is re-uptaken by the SERCA pumps to the SR. SERCA is regulated by SLN: a PKA-mediated phosphorylation of SLN increases the pump activity. A constitutive or agonist-mediated activation of CB1Rs activate $G\alpha_{i/o}$

proteins, decrease the activity of AC, thus reducing the concentration of cAMP, inactivating PKA. From here, two mechanisms are possible: 1.) RyR remains dephosphorylated and binds FKBP12 which decreases the open probability of RyR, allowing less Ca^{2+} release from the SR. 2.) The decreased phosphorylation of DHPR or RyR disrupts their interaction, resulting in a smaller Ca^{2+} release. SLN also remains dephosphorylated and attenuates the Ca^{2+} uptake via SERCA. The contribution of the βγ subunits of the G-proteins to this process seems to be negligible.
Colour code: red shows inactivation, while green shows activation of a protein as a consequence of CB1R activation. Abbreviations not used previously: AC: adenylyl cyclase; CSQ: calsequestrin; TnC: troponin-C.

Fig. 1

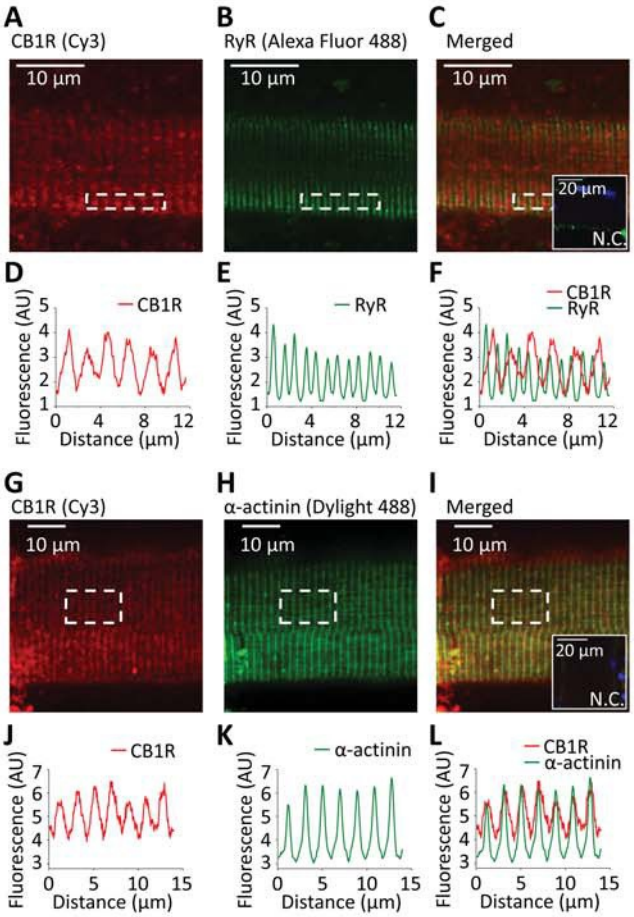
A
CB1R (Cy3)
10 µm
B
RyR (Alexa Fluor 488)
10 µm
C
Merged
10 µm
20 µm
N.C.
D
CB1R
Fluorescence (AU)
Distance (µm)
E
RyR
Fluorescence (AU)
Distance (µm)
F
CB1R
RyR
Fluorescence (AU)
Distance (µm)
G
CB1R (Cy3)
10 µm
H
α-actinin (Dylight 488)
10 µm
I
Merged
10 µm
20 µm
N.C.
J
CB1R
Fluorescence (AU)
Distance (µm)
K
α-actinin
Fluorescence (AU)
Distance (µm)
L
CB1R
α-actinin
Fluorescence (AU)
Distance (µm)

Fig. 2

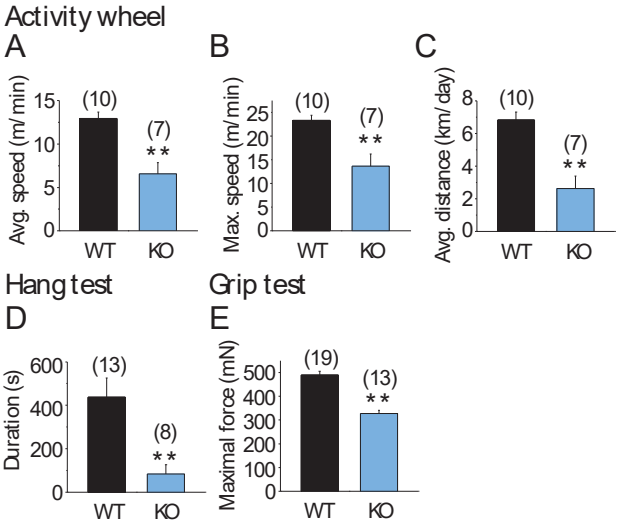
Activity wheel
A
Avg. speed (m/min)
15
10
5
0
(10)
(7)
**
WT
KO
B
Max. speed (m/min)
25
20
15
10
5
0
(10)
(7)
**
WT
KO
C
Avg. distance (km/day)
8
6
4
2
0
(10)
(7)
**
WT
KO
Hang test
D
Duration (s)
600
400
200
0
(13)
(8)
**
WT
KO
Grip test
E
Maximal force (mN)
500
400
300
200
100
0
(19)
(13)
**
WT
KO

Fig. 3

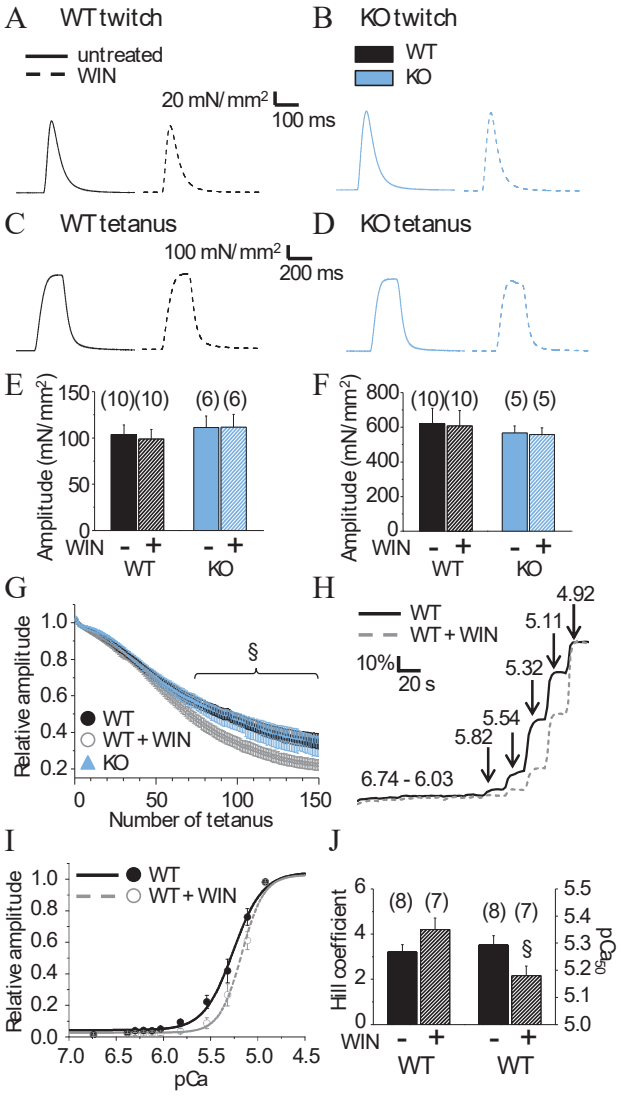
A
WT twitch
untreated
WIN
20 mN/mm2
100 ms
B
KO twitch
WT
KO
C
WT tetanus
100 mN/mm2
200 ms
D
KO tetanus
E
Amplitude (mN/mm2)
(10)(10)
(6) (6)
WIN
WT
KO
F
Amplitude (mN/mm2)
(10)(10)
(5) (5)
WIN
WT
KO
G
Relative amplitude
§
WT
WT + WIN
KO
Number of tetanus
H
WT
WT + WIN
10%
20 s
4.92
5.11
5.32
5.54
5.82
6.74 - 6.03
I
Relative amplitude
WT
WT + WIN
pCa
J
Hill coefficient
(8) (7)
(8) (7)
§
pCa50
WIN
WT
WT

Fig. 4

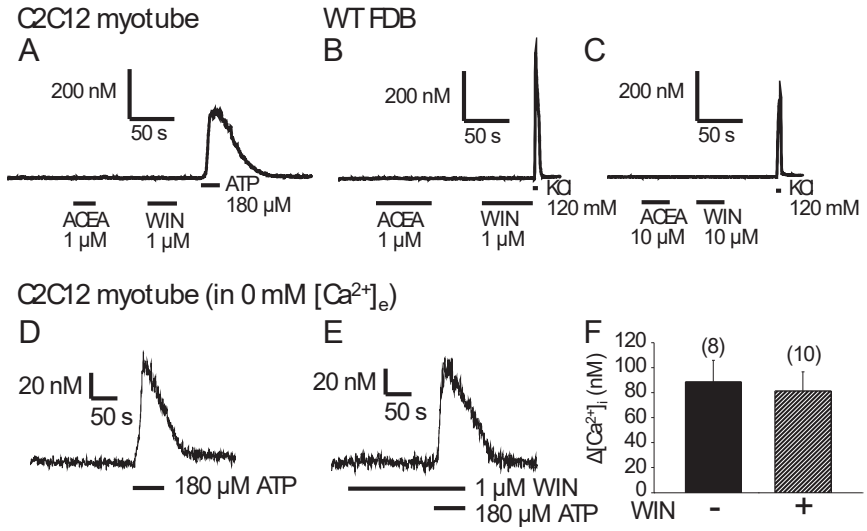
C2C12 myotube
A
200 nM
50 s
ATP
180 μM
ACEA
1 μM
WIN
1 μM
WT FDB
B
200 nM
50 s
KCl
120 mM
ACEA
1 μM
WIN
1 μM
C
200 nM
50 s
KCl
120 mM
ACEA
10 μM
WIN
10 μM
C2C12 myotube (in 0 mM [Ca2+]e)
D
20 nM
50 s
180 μM ATP
E
20 nM
50 s
1 μM WIN
180 μM ATP
F
Δ[Ca2+]i (nM)
120
100
80
60
40
20
0
(8)
(10)
WIN
-
+

Fig. 5

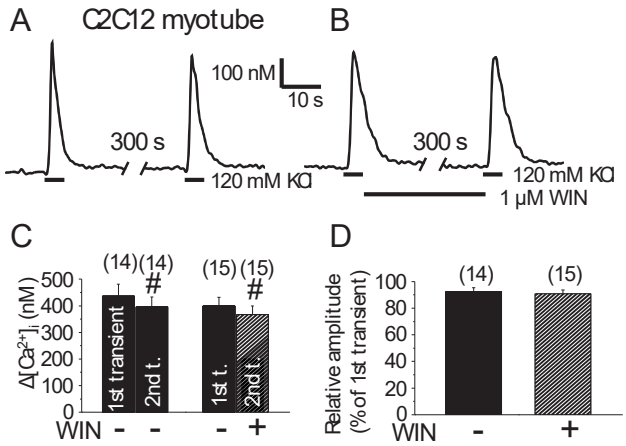
A
C2C12 myotube
B
100 nM
10 s
300 s
120 mM KCl
300 s
120 mM KCl
1 µM WIN
C
(14)(14)
(15)(15)
#
#
Δ[Ca2+]i (nM)
500
400
300
200
100
0
1st transient
2nd t.
1st t.
2nd t.
WIN - - - +
D
(14)
(15)
Relative amplitude (% of 1st transient)
100
80
60
40
20
0
WIN - +

Fig. 6

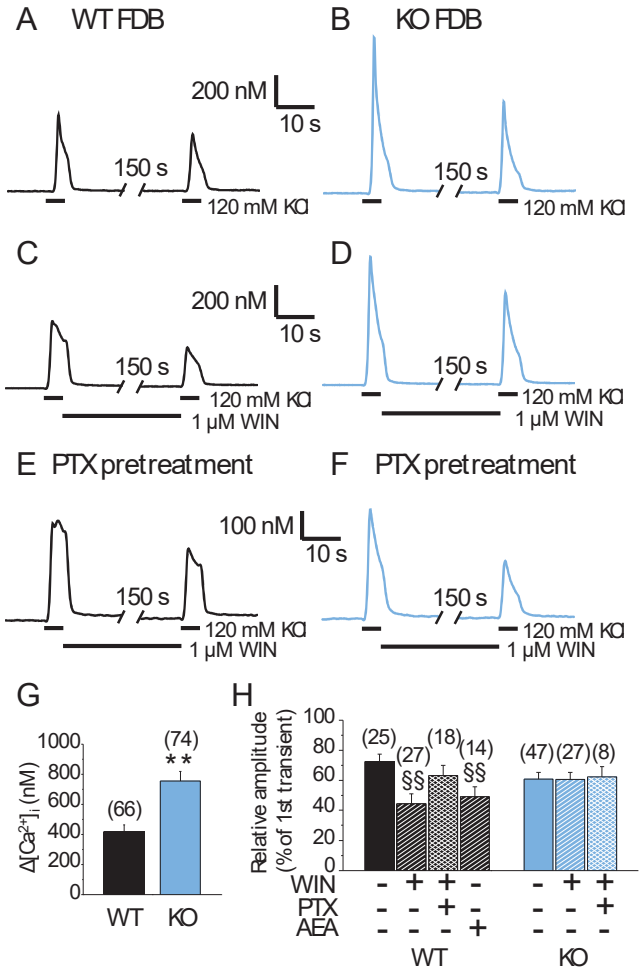
A WT FDB
B KO FDB
200 nM
10 s
150 s
120 mM KCl
C
D
1 µM WIN
E PTX pretreatment
F PTX pretreatment
100 nM
G
H
Δ[Ca2+]i (nM)
(66)
(74)
**
WT
KO
Relative amplitude (% of 1st transient)
(25)
(27)
(18)
(14)
(47)
(27)
(8)
§§
§§
WIN
PTX
AEA

Fig. 7

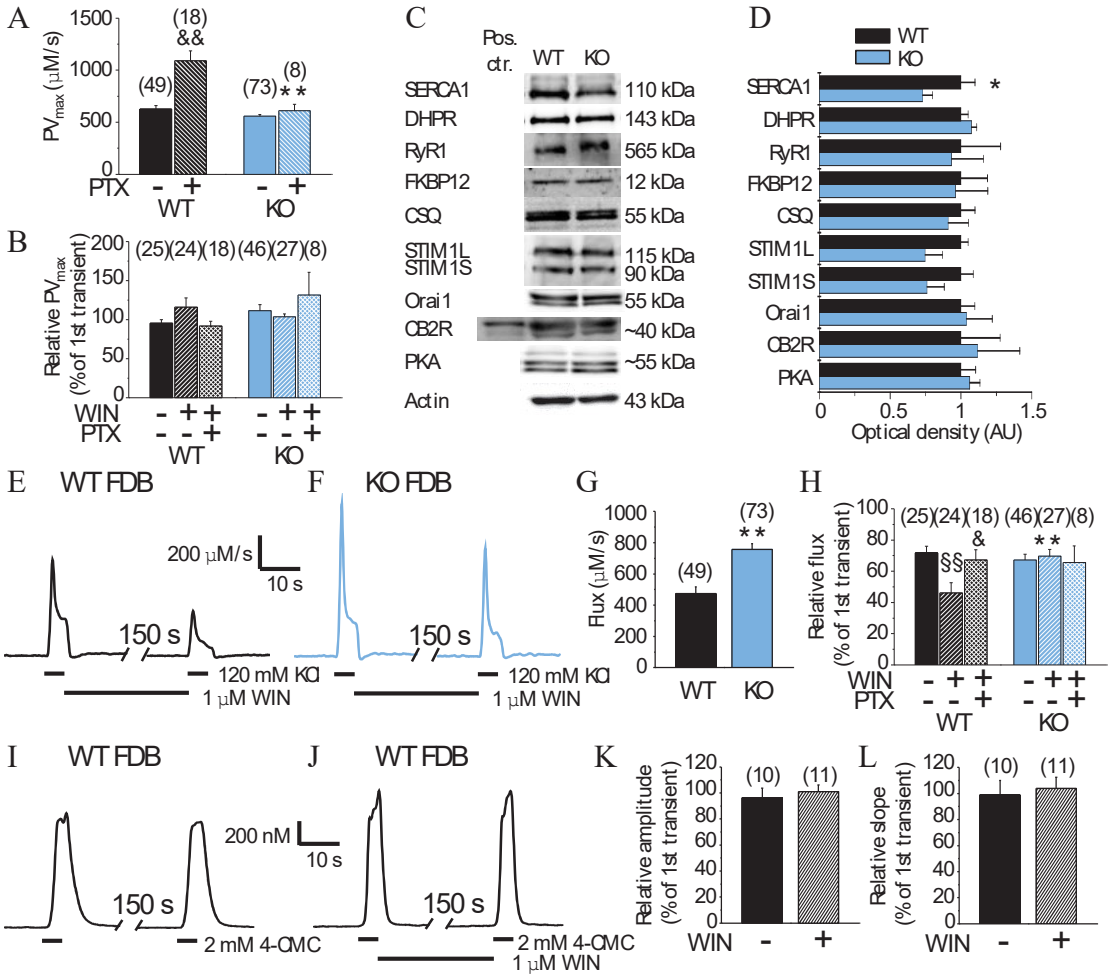
A
B
C
D
E WT FDB
F KO FDB
G
H
I WT FDB
J WT FDB
K
L
PTX
WT
KO
WIN
Pos. ctr.
SERCA1
DHPR
RyR1
FKBP12
CSQ
STIM1L
STIM1S
Orai1
CB2R
PKA
Actin
110 kDa
143 kDa
565 kDa
12 kDa
55 kDa
115 kDa
90 kDa
55 kDa
~40 kDa
~55 kDa
43 kDa
Optical density (AU)
200 µM/s
10 s
150 s
120 mM KCl
1 µM WIN
Flux (µM/s)
Relative flux
(% of 1st transient)
200 nM
2 mM 4-CMC
Relative amplitude
Relative slope

Fig. 8

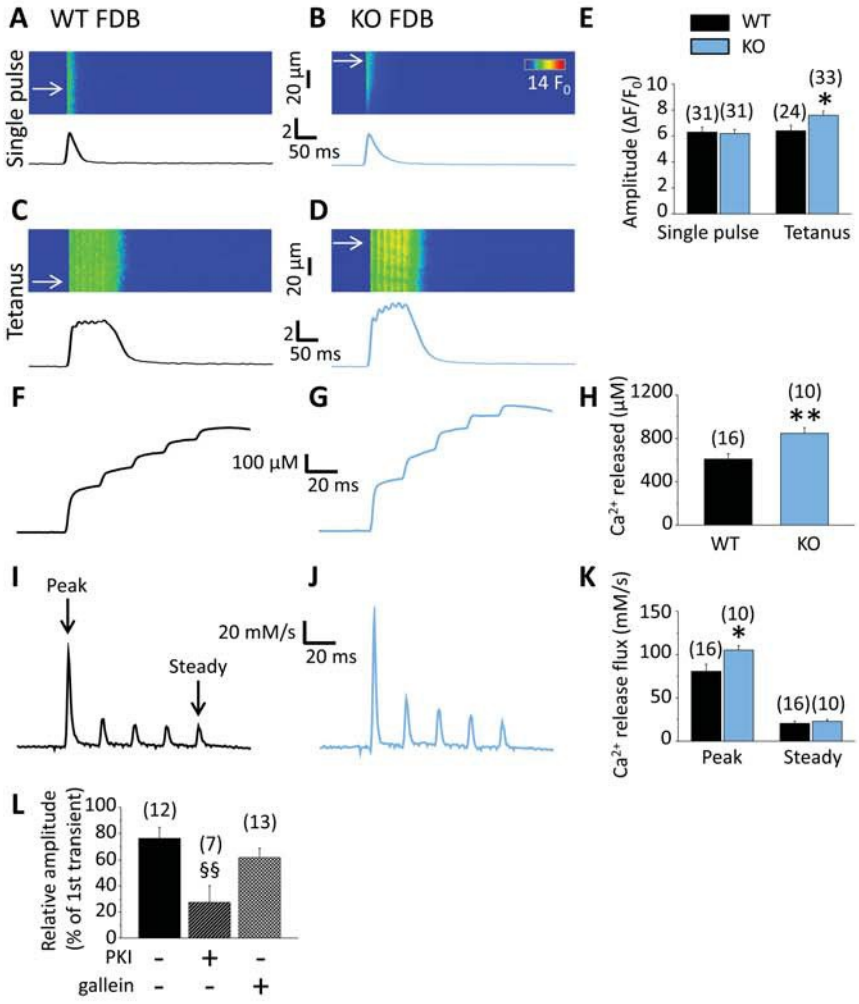
A WT FDB
B KO FDB
E
WT
KO
Single pulse
20 µm
14 F0
2
50 ms
Amplitude (ΔF/F0)
(31)(31)
(24)
(33)
*
Single pulse
Tetanus
C
D
Tetanus
F
G
100 µM
20 ms
H
Ca2+ released (µM)
(16)
(10)
**
WT
KO
I
Peak
Steady
J
20 mM/s
20 ms
K
Ca2+ release flux (mM/s)
(16)
(10)
*
(16)(10)
Peak
Steady
L
Relative amplitude (% of 1st transient)
(12)
(7)
§§
(13)
PKI
gallein

Fig. 9

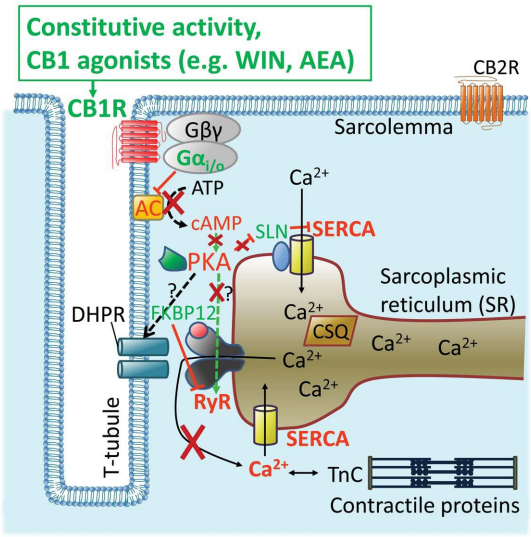
Constitutive activity,
CB1 agonists (e.g. WIN, AEA)
CB1R
CB2R
Sarcolemma
Gβγ
Gαi/o
ATP
AC
cAMP
PKA
SLN
SERCA
Ca2+
Sarcoplasmic
reticulum (SR)
DHPR
FKBP12
CSQ
RyR
T-tubule
TnC
Contractile proteins